STUB1-SMYD2 Axis Regulated Drug Resistance in Glioma cells

Kailing Pan (pankailingpan@126.com)
Jinhua Hospital of Zhejiang University: Jinhua Municipal Central Hospital
Bin Hu
Jinhua Hospital of Zhejiang University: Jinhua Municipal Central Hospital
Lude Wang
Jinhua Hospital of Zhejiang University: Jinhua Municipal Central Hospital
Jinyong Fang
Jinhua Guangfu Oncology Hospital
Jianlie Yuan
Jinhua Hospital of Zhejiang University: Jinhua Municipal Central Hospital
Wenxia Xu
Jinhua Hospital of Zhejiang University: Jinhua Municipal Central Hospital

Research Article

Keywords: SMYD2, gliomas, drug resistance, STUB1

Posted Date: October 22nd, 2021

DOI: https://doi.org/10.21203/rs.3.rs-968469/v1

STUB1-SMYD2 Axis regulated Drug Resistance in Glioma cells

Kailing Pan[1†], Bin Hu[2†], Lude Wang[1], Jinyong Fang[3], Jianlie Yuan[4*], Wenxia Xu[1*]

1. Central Laboratory, Affiliated Jinhua Hospital, Zhejiang University School of Medicine, Jinhua 321000, Zhejiang Province, China
2. Department of Pathology, Affiliated Jinhua Hospital, Zhejiang University School of Medicine, Jinhua 321000, Zhejiang Province, China.
3. Department of science and education, Jinhua Guangfu Oncology Hospital, Jinhua 321000, Zhejiang Province, China
4. Department of Neurosurgery, Affiliated Jinhua Hospital, Zhejiang University School of Medicine, Jinhua 321000, Zhejiang Province, China.

***Correspondence:**

Corresponding Author

Xuwenxia@zju.edu.cn, yuanjianlie@zju.edu.cn

[†]These authors contributed equally to this work.

Author Declarations

Ethics approval and consent to participate: This study was carried out in accordance with the recommendations in the Guide for the Care and Use of Laboratory Animals of the National Institutes of Health, and the corresponding protocol was approved by the Medical Ethics Committee of Jinhua Central Hospital (Jinhua, Zhejiang Province, China).

Consent for publication: The authors agree for publication.

Availability of data and materials: The data and materials are available.

Competing Interests: The authors declare that the research was conducted in the absence of any commercial or financial relationships that could be construed as a potential conflict of interest.

Funding: This work was supported by Key Research and Development Program of Zhejiang Province (2019C03044), Jinhua Science and Technology Research Program (2017-3-006, 2020-3-046, 2020-3-049), Natural Science Foundation of Zhejiang province

(LY21H160014), Foundation of Jinhua hospital (JY2019-3-001, JY2020-6-04).

Author Contributions: KP: carried out the experiments and wrote the manuscript. BH: tissue microarray. LW: assisted with the experiments. JF: assisted with analyzed the experimental results. JY and WX: designed the experiments and modified the manuscript. All authors contributed to the article and approved the submitted version.

Acknowledgements: Not applicable

Compliance with Ethical Standards

Disclosure of potential conflicts of interest: The authors declare that the research was conducted in the absence of any commercial or financial relationships that could be construed as a potential conflict of interest.

Research involving Human Participants and/or Animals: This study was carried out in accordance with the recommendations in the Guide for the Care and Use of Laboratory Animals of the National Institutes of Health, and the corresponding protocol was approved by the Medical Ethics Committee of Jinhua Central Hospital (Jinhua, Zhejiang Province, China).

Informed consent: The informed consent has been uploaded as an attachment.

Abstract

Aim: SMYD2 is an important epigenetic regulator that methylates histone and non-histone proteins. This study aims to investigate SMYD2 as an oncogene of gliomas and explore its degradation mechanism induced by cisplatin.

Methods: Tumor tissue microarray of 441 glioma patients was collected for SMYD2 immunohistochemistry staining. Kaplan-Meier survival curves were constructed by using the overall survival. mRNA-sequencing analysis was detected for understanding the downstream mechanisms mediated by SMYD2. The half-inhibitory concentrations (IC50) of temozolomide and cisplatin in AZ505-treated and control cells were calculated. The potential E3 ubiquitin ligase of SMYD2 was predicted in UbiBrowser and confirmed by

knockdown test. The effect of SMYD2 and its E3 ligase on gliomas apoptosis and migration were determined via cell-function assays.

Results: High SMYD2 expression correlated with a high WHO stage (P=0.004) and a low survival probability (P=0.012). The inhibition of SMYD2 suppressed the process of EMT by downregulating the expression of COL1A1. AZ505 treatment significantly increased drug sensitivity of glioma cells. And the expression of SMYD2 was markedly reduced by cisplatin treatment via STUB1 mediated degradation. The knockdown of STUB1 could partly reverse the cell function impairment induced by cisplatin.

Conclusion: These findings suggested that SMYD2 could be a potential drug target for the treatment of gliomas, and STUB1-mediated degradation of SMYD2 plays an important role in reversing chemotherapy resistance in gliomas.

Keywords: SMYD2, gliomas, drug resistance, STUB1

Introduction

Gliomas are the most common form of malignant primary brain tumors in adults(Ostrom et al., 2016). Due to its aggressive nature and evasiveness to standard first line treatment with combinations of radiation and chemotherapy, gliomas display a poor prognosis with median survival less than 2 years in patients after treatment(Tan et al., 2020). Therefore, understanding the molecular mechanisms that control glioma progression and drug resistance is imperative and important for the establishment of new strategies in its clinical treatment.

SET and MYND domain-containing protein 2 (SMYD2) is a member of the SMYD-methyltransferase protein family that methylates histone at lysine 36 (H3K36) and nonhistone proteins such as P53, RB1 and PTEN (Brown et al., 2006; Huang et al., 2006; Saddic et al., 2010; Nakakido et al., 2015). SMYD2 is most highly expressed in heart tissue, acting as an important role in cardiomyocyte survival and cardiac function(Brown et al., 2006; Sun et al., 2020). And as an oncogene, SMYD2 overexpressed in a wide range of cancer including breast, ovarian and renal, and knockdown or inhibition of SMYD2 suppresses tumor cell growth by methylating different substrates(Kukita et al.,

2019; Song et al., 2019; Yan et al., 2019). For example, SMYD2 promotes breast cancer cell growth by methylating ERα and PTEN, resulting in AKT activation, and in bladder cancer, RB is methylated by SMYD2 (Cho et al., 2012; Zhang et al., 2013; Nakakido et al., 2015). In addition, previous studies also reported that SMYD2 affects the drug resistance in non-small cell lung cancer and esophageal squamous cell carcinoma. AZ505 is an effective and highly selective, competitive inhibitor of SMYD2 that binds in the peptide-binding groove of SMYD2(Ferguson et al., 2011).

E3 ligases are a class of enzymes that can transfer ubiquitin to substrates for their degradation, which are of importance in cellular homeostasis. Intriguingly, many oncogenic proteins were reported to be regulated by the E3 ligase, attracting more and more attentions as promising anticancer targets(Wang et al., 2017). However, the E3 ligases modulating SMYD2 degradation remain unknown.

Till date, little is known about the role of SMYD2 in glioma. In this study, we showed that SMYD2 expression levels were significantly increased in high-grade serious gliomas, and high SMYD2 expression is correlated with a poor prognosis. Further study indicated that the inhibition of SMYD2 promoted sensitivity of glioma to chemotherapy drugs. And the expression of SMYD2 was significantly reduced following cisplatin treatment which was mediated by STUB1. Additionally, the knockdown of STUB1 attenuates the anticancer effect of cisplatin in glioma. Our results provide a potential target for the therapeutic strategies of glioma.

Materials and methods

Patients and tissue samples

Tumor tissue microarray was afforded by the Affiliated Hospital of Xuzhou Medical University. All patients involved in this study provided written informed consent. According to the WHO, the tumors were divided according to the pathological grade as follows: 237 cases with grades Ⅰ-Ⅱ and 195 cases with grades Ⅲ-Ⅳ.

Immunohistochemistry (IHC) and histopathological assessments

IHC was uniformly performed to evaluate the SMYD2 protein expression in the glioma

samples. Samples using the Bond Polymer Refine Detection System (Leica Biosystems, Wetzlar, Germany). The immune-reactive score (IRS), which represents the intensity and quantity the stained cells, was implemented to quantify the staining level of SMYD2. The SMYD2 staining intensity was scored as follows: 1, negative; 2, weak; 3, moderate; and 4, strong. The proportion of the positively stained cells was defined as follows: 1, 0%-25%; 2, 26%-50%; 3, 51%-75%; 4, 76%-100%. The immunoreactive score (IRS) was calculated by multiplying the score of the staining intensity and the proportion of positive cells. Samples with an IRS score of <=4 was considered as those with low SMYD2 expression and samples with an IRS score of >5 was considered as those with high SMYD2 expression.

Cell Lines and Cell Culture

U251 and U87 human glioma cell lines were purchased from the Cell Bank of the Type Culture Collection Committee of the Chinese Academy of Sciences. These glioma cells were cultured in DMEM medium supplemented with 10% fetal bovine serum and were maintained at 37℃ in a humidified incubator with 5% CO_2.

Antibodies, reagents and plasmid

Antibodies against the following proteins were used: γ-H2AX (ab81299) from Abcam (Cambridge, UK); Histone H3 (4499) and Di-Methyl-Histone H3 (Lys 36) (2901) from Cell Signaling Technology (Danvers, MA, USA); SMYD2 (21290-1-AP) from Proteintech (Rosemont, IL, USA); Methyl P53 (Lys 370) from Immunoway Biotechnology (Plano, TX, USA); GAPDH (AG019), Bax (AF1270), Bcl2 (AF6285), CyclinD1 (AF1183), P53 (AF1162), COL1A1 (AF6524), N-Cadherin (AF5237) and E-Cadherin (AF6759) from Beyotime Biotechnology (Shanghai, China). The following reagents were used in this research: AZ505 (HY-15226), Cisplatin (HY-17394) and Temozolomide (HY-17364) from MedChemExpress (Monmouth Junction, NJ, USA). Plasmid of SMYD2 (HG11093-NF) was purchased from SinoBiological (Beijing, China).

Quantitative reverse transcription PCR (RT-qPCR)

To evaluate the differentially expressed mRNAs in AZ505-treated cells relative to control cells, total cellular RNA was extracted using TRIzon reagent (CW0580, Cwbio, Beijing, China) and cDNAs were synthesized using PrimeScript™ RT Master Mix (RR036A, Takara). Realtime PCR was performed using SYBR Green Realtime PCR Master Mix (RR430, Takara) and Cobas z 480 (Roche, Basel, Switzerland). The primers for SMYD2, BAX, GADD45, P21, COL1A1, MMP7 and β-actin were synthesized by TSINGKE Biological Technology (Beijing, China). β-actin was served as an internal reference of RNA integrity. The sequences are as follows:

SMYD2-F 5'-CTCCAAGCATCTCGGATTCCC-3'

SMYD2-R 5'-TGCAACATCAGGAAATATCGCTG-3'

BAX-F 5'-TTTGCTTCAGGGTTTCATCC-3'

BAX-R 5'-CAGTTGAAGTTGCCGTCAGA-3'

GADD45-F 5'-GGATGCCCTGGAGGAAGTGCT-3'

GADD45-R 5'-GGCAGGATCCTTCCATTGAGATGAATGTG-3'

P21-F 5'-TGTACCCTTGTGCCTCGCTC-3'

P21-R 5'-TGGAGAAGATCAGCCGGCGT-3'

COL1A1-F 5'-GAAGACATCCCACCAATCACC-3'

COL1A1-R 5'-TCGTCACAGATCACGTCATCG-3'

MMP7-F 5'-ACAGGCTCAGGACTATCTCAAG-3'

MMP7-R 5'-ACATTCCAGTTATAGGTAGGCC-3'

β-actin-F 5'-ACTCTTCCAGCCTTCCTTCC-3'

β-actin-R 5'-CGTCATACTCCTGCTTGCTG-3'

Western blot

The cells were harvested and rinsed twice with PBS. All protein samples were denatured and separated on 8-12% SDS-polyacrylamide gels and transferred to polyvinylidene fluoride membranes. Membranes were blocked with 5% milk in T-BST at room temperature for 1 h and incubated with primary antibody overnight at 4 ℃. After washing 3 times with T-BST, membranes were incubated with secondary antibodies for 1 h at room

temperature. Proteins visualized using the Electrochemiluminescence (ECL) and detected in The ChemiDoc MP system (Bio-Rad, Hercules, USA).

Migration assays

This assay was conducted using a transwell chamber (3422, Costar) with a pore size of 8 μm. The upper chamber was filled with $5x10^4$ cells in a serum-free medium. After incubation for 24 h for migration, the cells in the upper chamber were carefully removed with a cotton swab, the cells that traversed in the membrane were fixed in methanol and stained with crystal violet, and the permeating cells were calculated and photographed under light microscopy.

Cell proliferation assay

Cells were plated onto 96-well plates at a density of 2000 cells per well. After 24 h, cells were treated with DMSO or AZ505 and then cultured for 24, 48, 72 and 96 h, respectively. At the same time point on these 4 days, CCK-8 solution (C0042, Beyotime Biotechnology, China) was added to the wells needed to be measured. After incubation for 1 h at 37 ˚C, the proliferation rate was evaluated based on the increase in the absorbances at 450 nm.

Wound healing assay

Cells were plated onto 6-well plates at 100% density and cultured for 24 h. Then a rectangular lesion was created using a plastic pipette tip, and the monolayer was irrigated twice with PBS and incubated in serum-free media with AZ505 or DMSO. At the designated time, nine randomly selected fields at the lesion border were determined for shooting under an inverted microscope.

Cell apoptosis assay

Cells were plated onto 6-well plates at a density of 70-80% for 24 h. For analyzing the apoptosis induced by AZ505, cells were treated with DMSO or AZ505. For analyzing drug sensitivity induced by AZ505, cells were treated with DMSO, cisplatin or the combination of AZ505 and cisplatin. For analyzing drug resistance induced by the knockdown of STUB1, cells were treated with si-NC or si-STUB1 for 24 h, then cells were treated with

DMSO or cisplatin. After 24 h, cells were collected and were marked using 300 μL Annexin V-FITC binding reagent containing 6 μL propidium iodide (PI) and 3 μL Annexin V-FITC (C1062L, Beyotime Biotechnology, China) for 15 min at room temperature. The apoptosis rate was measured using a Flow cytometer (EasyCell 204A1/206A1, Wellgrow, China).

Active oxygen detection assay

Cells were plated onto 6-well plates at a density of 70-80% for 24 h. For analyzing the apoptosis induced by AZ505, cells were treated with DMSO or AZ505. For analyzing drug sensitivity induced by AZ505, cells were treated with DMSO, cisplatin or the combination of AZ505 and cisplatin. After 24 h, cells were collected and washed for 3 times using PBS. 500 μL DMEM containing 10 μM DCFH-DA was added to cells. The mixture was incubated at 37 ˚C for 20 min and then washed using PBS for 3 times to fully remove the DCFH-DA that has not entered the cells. Cells were resuspended using 300 μL PBS. And the active oxygen level was detected using a Flow cytometer (EasyCell 204A1/206A1, Wellgrow, China).

Bioinformatics analyses

AZ505-treated and control U251 cells were collected for RNA sequencing conducted by CapitalBio corporation (Beijing, China). Limma package in the R software was used for the differential mRNA expression analysis. Significantly dysregulated mRNAs were defined using a cutoff $|\log_2$fold-change$|$ value of >1 and P value of <0.05. The identified differential expressed genes (DEGs) were subjected to both Gene Ontology (GO) and Kyoto Encyclopedia of Gene (KEGG) pathway analyses using ClusterProfiler package. And the Gene Set Enrichment Analysis (GSEA) were analyzed using all detected genes on the GSEA software (version 4.1.0). The protein-protein interaction (PPI) analysis was produced in STRING website (https://string-db.org/), and the results were then imported into Cytoscape software (https://www.cytoscape.org). ClueGo app was used to GO and KEGG pathway analyses. Then, hub genes were predicted using degree algorithm of cytoHubba app. The prognostic values of these hub genes were assessed in GEPIA2

website (http://gepia2.cancer-pku.cn/#index).

The prognostic analysis of SMYD2, COL1A1 and STUB1 were assessed in GEPIA2 and CGGA website (http://cgga.org.cn/index.jsp). The expression level in different stage of glioma of SMYD2, COL1A1 and STUB1 were analyzed in CGGA website.

Statistical analysis

Statistical analyses were performed using the GraphPad Prism 9 for Mac (GraphPad Prism Software Inc., San Diego, CA, USA). Comparisons between two groups were performed using an unpaired Student's t test. One-way analysis of variance (ANOVA) followed by post-hoc test was used for multiple comparisons. These data are presented as the means ± standard deviations (SDs), and $P < 0.05$ was considered to reflect a statistically significant difference.

Results

SMYD2 expression was correlated with survival in glioma

To determine whether or not the SMYD2 expression is associated with survival in glioma, we performed the Keplan-Meier survival analysis based on the expression of SMYD2 in GEPIA2 and CGGA databases. The result in GEPIA2 database (http://gepia2.cancer-pku.cn) showed that SMYD2 expression levels in glioma were significantly associated with a worse overall survival (OS, $p<0.0001$, Fig. 1A) and disease-free survival (DFS, $p<0.0001$, Fig.1B). Similarly, the results in CGGA database (http://www.cgga.org.cn) showed that the high expression of SMYD2 is not only related to a worse overall survival in primary glioma patients ($p<0.0001$, Fig. 1C), but also has a significant correlation in recurrent glioma patients ($p=0.0059$, Fig. 1D). In addition, the SMYD2 expression levels for the glioma samples in the CGGA database were compared, the results indicated that the SMYD2 expression was significantly positively associated with the WHO grade (Fig. 1E).

To further confirm these findings in protein level, we performed immunohistochemical staining in 441 pathologically confirmed glioma tissues. SMYD2 was widely distributed in

the nucleus and cytoplasm of the glioma cells. According to the intensity and quantity scores of the staining, glioma samples were divided into the high SMYD2 expression (n=214) and low SMYD2 expression (n=227) groups. The specific and representative IHC-staining intensity patterns for the SMYD2 protein in the glioma samples are shown in Figure 1F. The Kaplan-Meier survival curves were constructed by using the overall survival; the result showed that the high expression group had a shorter survival time than the low expression group (p=0.012, Fig. 1G). In addition, we also analyzed the associations between the SMYD2 expression levels and clinicopathological parameters. Table 1 showed that high SMYD2 expression was significantly correlated with a higher WHO grade (p=0.004) but not with patient's age, gender, and histological type. Together, these results suggested that SMYD2 may act as an oncogene and high SMYD2 expression predicted poor survival in patients with glioma.

SMYD2 inhibition suppressed cell proliferation and promoted cell apoptosis

To explore and verify the function of SMYD2 as a potential oncogene in glioma, we first estimated the IC_{50} values of AZ505 for U251 and U87 cells. The estimated IC_{50} value for U251 was about 8 μM while U87 was about 10 μM (Fig. 2A). We further investigated whether the inhibition of SMYD2 could induce cell apoptosis. After 24 h of AZ505 or vehicle treatment, cells were collected for cell apoptosis assay. The flow cytometer data showed that compared with the corresponding controls, SMYD2 inhibition significantly increased the apoptosis rate by 50% in U251 and U87 cells (Fig. 2B-C).

We then investigated the role of SMYD2 in glioma migration by wound healing and transwell assays in U251 and U87 cells. The results of wound-healing assays showed that the capabilities of migration were significantly reduced in two cell lines with SMYD2 inhibition compared to the corresponding controls (Fig. 2D-E). And the transwell assays were continue validated the finding in wound-healing assays. After 24 h, the number of AZ505-treated cells detected on lower layer were decreased by 50-70% compared to control cells (Fig. 2F-G). Given that cell apoptosis and migration were controlled by the activity of SMYD2, we performed cell proliferation assays in glioma cells. The results demonstrated that the growth rate was significantly decreased after the inhibition of

SMYD2 via AZ505 treatment in both U251 and U87 cells (Fig. 2H-I). In addition, active oxygen detection assay showed that the inhibition of SMYD2 slightly increased the level of active oxygen (Fig. S1). Altogether, these results indicated that SMYD2 plays an important role in controlling cells proliferation, migration and the inhibition of SMYD2 wound leads to cell apoptosis.

The downstream mechanisms induced by SMYD2 inhibition

To gain insight into the molecular events underlying SMYD2 inhibition, we first verified the methylation levels of the downstream molecules, P53 and H3K36, which identified in previous studies(Brown et al., 2006; Huang et al., 2006). Western blot analysis showed that AZ505 treatment significantly reduced the methylation levels of P53 and H3K36 (Fig. 3A). The mRNA levels of P21, GADD45 and Bax were upregulated after the inhibition of SMYD2 (Fig. 3B). In addition, CyclinD1 protein level was significantly downregulated, the ratio of Bax/Bcl2 and the level of γH2AX were upregulated (Fig. 3A), indicating that SMYD2 inhibition activated P53 pathway leading to DNA damage, cell cycle arrest and cell apoptosis.

Then mRNA-sequencing analysis was used to identify the specific mechanisms induced by SMYD2 inhibition in glioma cells. The DEGs showing statistical significance between control and AZ505 treated cells was screened according to the criteria of $P<0.05$ and $|\log FC|>1$. The integral gene expression variation was visualized by volcano plots. As shown in Fig. 3C, a total of 105 genes displayed differential expression, including 58 upregulated genes and 47 downregulated genes. Heatmap was used to demonstrate the profiles of the identified DEGs using hierarchical clustering analysis to reflect the state of the cells (Fig. S2. A). Functional classification of identified DEGs was conducted using GO, KEGG and GSEA enrichment analysis. The biological process (BP) analysis showed that genes related to *steroid metabolic process* were upregulated while genes associated with *epithelial to mesenchymal transition (EMT)* were downregulated (Fig. 3D). The KEGG analysis showed that the inhibition of SMYD2 disturbed the gene expressions of several pathways including *Steroid biosynthesis*, *IL-17 signaling pathway* and *Transcriptional*

misregulation in cancer (Fig. 3E). And GSEA analysis showed that changes of the gene set of *Steroid biosynthesis* is the most significant (Fig. 3F).

Proteins often function by protein-protein interactions (PPI), which is essential for almost all biochemical activities. For deeply understanding the regulatory mechanisms in SMYD2 inhibition, we performed PPI analysis based on the identified DEGs. The identified DEGs were mapped to STRING for PPI analysis. The PPI network, which contains 123 edges for a total of 55 nodes, was imported into Cytoscape for further analysis (Fig. S2. B). The GO-BP and KEGG analysis were conducted using ClueGo. As shown in Fig. 3G, the PPI network predominantly involved *Regulation of Steroid metabolic process*, *ER-nucleus signaling pathway* and *Regulation of epithelial to mesenchymal transition*. And *Steroid biosynthesis*, *IL-17 signaling pathway* and *Transcriptional misregulation in cancer* pathways had also been identified in KEGG analysis (Fig. 3H). Hub genes were selected using the degree algorithm of cytoHubba (Fig. 3I) and performed the Keplan-Meier survival analysis in GEPIA2 database (Table 2). H3K36 methylation of SMYD2 is an activating modification; thus, we focused on genes that were downregulated after SMYD2 inhibition. Two genes, COL1A1 and MMP7, were expressed lower than normal cells in AZ505 treated cells. And the high expression levels of these two genes both associated with a worse overall survival (Table 2). To confirm these results, we performed qPCR in both U251 and U87 cells treated with AZ505. The results showed that the expression of COL1A1 significantly reduced in U251 and U87 cells whereas MMP7 increased in U87 (Fig. 3J). COL1A1 is the major component of the process of EMT(Wang et al., 2020b), which was the process identified in GO enrichment analysis after the treatment of AZ505 in U251 cells. To confirm the role of SMYD2 in modulating the EMT process, we examined the expression of EMT related proteins after inhibiting SMYD2 in glioma cells. The results showed that the inhibition of SMYD2 decrease the expression of COL1A1 and N-Cadherin (Fig. 3K). Together, our results indicated that SMYD2 inhibition suppressed the process of gliomas through various pathways including the activation of P53 signaling pathway and Steroid biosynthesis and the inhibition of EMT process.

Inhibition of SMYD2 enhanced drug sensitivity in glioma

The reason that glioma is difficult to treat relates not only a restriction in the total amount of tumor mass that can be safely removed, but also to resistance against adjuvant therapy after surgical resection. Temozolomide and Cisplatin are commonly used in the treatment of glioma. To verify whether SMYD2 inhibitor enhanced sensitivity of glioma cells to drugs, the IC_{50} values of temozolomide and cisplatin for AZ505-treated cells and control cells were estimated. The estimated IC50 values of both temozolomide and cisplatin for AZ505-treated glioma cells were significantly lower than those for the control cells (Fig. 4A). Next, the flow cytometer analysis, wound healing analysis and active oxygen detection assay were used to evaluate the synergistic effects of AZ505 and Cisplatin. Following the combination treatment with AZ505 and Cisplatin, the apoptosis rate and the level of active oxygen were significantly increased while the migration rate were reduced (Fig. 4B-G). These results indicated that the SMYD2 inhibition enhanced the drug sensitivity in glioma.

To identify whether the antitumor efficacy of Cisplatin effect partly through SMYD2, we examined the expression of SMYD2 in cisplatin treated cells. The expression level of SMYD2 in cisplatin-treated cells significantly lower than control cells and this downregulation was associated with higher concentrations of cisplatin (Fig. 4H). And after cisplatin treatment, the expression of SMYD2 first increased and then decreased, indicating that SMYD2 first participated in the regulation of the stress process to cisplatin and then the degradation of SMYD2 may induced cell apoptosis (Fig. 4I).

STUB1 modulated SMYD2 degradation

To identify the mechanisms of the downregulation of SMYD2 induced by cisplatin in glioma cells, we detected the mRNA level after cisplatin treatment. The mRNA showed a slightly decrease after cisplatin treatment, indicating that the transcription of SMYD2 was not modulated by cisplatin (Fig. S3. A). Then the degradation rate of SMYD2 was examined. Following CHX treatment, the expressions of SMYD2 at different time in cisplatin-treated cells and control cells were detected. The degradation of SMYD2 was observed at 2 h in cisplatin-treated cells whereas 4 h in control cells (Fig. 5A-B). Furthermore, the decrease of SMYD2 induced by cisplatin was reversed by MG132 (Fig.

5C). The potential E3 ubiquitin ligases of SMYD2 was predicted using UbiBrowser (http://ubibrowser.ncpsb.org/) , of which FZR1 and STUB1 were showed higher scores (Fig. 5D). FZR1 and STUB1 were knocked down using siRNAs in U251 cells. As shown in Fig. 5E and Fig. S3. B, the mRNA levels of FZR1 and STUB1 were significantly reduced by siRNAs. And the expression of SMYD2 was significantly upregulated after the knockdown of STUB1 rather than FZR1 (Fig. 5F, Fig. S3. C). In addition, co-immunoprecipitation analysis revealed that SMYD2 and STUB1 could interact with each other in glioma cells (Fig. 5G). And the knockdown of SMYD2 could virtually reverse the downregulation of SMYD2 induced by cisplatin (Fig. 5H). Altogether, our results indicated that cisplatin promoted the degradation of SMYD2 via STUB1.

STUB1 knockdown reverse the effect of cisplatin

To elucidate the association of STUB1 with the survival of glioma, the Keplan-Meier survival analysis was performed in GEPIA2 and CGGA databases. Contrary to SMYD2, STUB1 expression levels in glioma were positively correlated with the survival prognosis of patients in glioma, and it decreased with a higher WHO grade (Fig. 6A-B). The biological phenotypes analysis showed that the knockdown of STUB1 could slightly protect cells from being killed by cisplatin and significantly promoted the migration rate of glioma cells (Fig. 6C-F). What's more, the knockdown of STUB1 also reversed the mis-regulation of the EMT-related proteins including COL1A1 and N-Cadherin (Fig. 6G). Therefore, STUB1 may act as a tumor suppressor partially restored the damage induced by cisplatin in glioma.

Altogether, as shown in Fig. 6H, our results indicated that SMYD2 could promote the progress of gliomas through several downstream pathways including *P53 signaling pathway*, *Steroid biosynthesis* and *EMT*. After the treatment of Cisplatin, SMYD2 was degraded via STUB1-mediated ubiquitin proteasome pathway, which led to cell death in gliomas.

Discussion

SMYD2 is a putative oncogene that affects the proliferation, migration, apoptosis and

chemosensitivity of tumor cells. Previous studies showed that SMYD2, as a prognostic marker, was overexpressed in various cancers including renal cell carcinoma, lung cancer, gastric cancer and bladder cancer(Komatsu et al., 2015; Xu et al., 2018; Shang and Wei, 2019; Yan et al., 2019). And accumulating evidence indicated that SMYD2 was associated with drug resistance of human cancers(Xu et al., 2018; Shang and Wei, 2019). In this study, SMYD2 was found to be a risk factor in gliomas, patients with higher SMYD2 expression showed a poor prognosis in the database of GEPIA and CGGA and our cohort of 441 gliomas cases. And the SMYD2 expression in glioma tissues is significantly positively associated with the WHO grade.

P53 plays a prominent role in controlling the cell cycle and apoptotic demise of gnomically compromised cells through activating its downstream molecules such as P21, GADD45 and BAX (Tomiyama and Ichimura, 2019). The activity of P53 was regulated by methylation. Previous studies reported that Set7/9 stabilized and activated P53 by dimethylating Lys372 of P53 whereas SMYD2 suppressed the activity of P53 by monomethylating P53 at 'Lys-370'(P53K370me1)(Huang et al., 2006; Ivanov et al., 2007; Chen et al., 2019). Here, we reported that the inhibition of SMYD2 activated P53 signaling pathway in glioma cells, which were confirmed by the upregulation of P21, GADD45, BAX and H2AX and the downregulation of CyclinD1.

Steroids, including cholesterol and steroid hormones, are involved in numerous cell biological processes, among which cholesterol is an essential lipid component of cell membrane, maintaining membrane integrity and fluidity(Espinosa et al., 2011). Cholesterol can be synthesized from acetyl-CoA through nearly 30 enzymatic reactions, in which 3-hydroxy-3-methylglutaryl-CoA (HMG-CoA) reductase (HMGCR) and squalene epoxidase (SQLE) are the two-key rate-limiting enzymes(Göbel et al., 2020). In addition, cholesterol can be acquired by the LDL hydrolyzation, which absorbed from blood circulation through LDL receptors (LDLR)(Wijers et al., 2015). In recent years, increasing evidence showed that cholesterol metabolism act as signal pathways promoting tumor development(Xu et al., 2020). For example, studies showed that the augmented level of HMGCR are associated with the growth and migration of gliomas and the upregulation of LDLR could promote cell survival(Guo et al., 2011; Qiu et al., 2016). Here, our results

showed the enhanced expression of LDLR, HMGCR and SQLE in U251 cells after AZ505 treatment. And the functional enrichment analysis, including GO, KEGG and GSEA enrichment analysis, also displayed the enhancement of *Steroid biosynthesis*. Combined with the restraint of cell function in AZ505 treated cells, we speculated that the up regulation of genes related to *Steroid biosynthesis* may be a negative feedback effect of cells in response to cholesterol degradation. However, the specific regulation mechanisms needed to be further studied.

EMT is the process that epithelial cells lose the apical-basal polarity and cell-cell adhesion, and transit to invasive mesenchymal cells. Cells undergoing EMT displayed decreased expression level of epithelial genes (such as E-cadherin and ZO-1), and increased expression level of mesenchymal genes (such as N-cadherin and vimentin), leading to numerous phenotypic changes (such as loss of adhesion and gain of stem cell-like features)(Du and Shim, 2016). Several signaling pathways, including TGFβ, Wnt and Notch, are participated in the modulation of EMT, of which the activation of TGFβ pathway can induce the expression of the mesenchymal genes (such as vimentin)(Gonzalez and Medici, 2014; Wei et al., 2019; Su et al., 2020; Wang et al., 2020a). In this study, mRNA-Seq results showed that the inhibition of SMYD2 significantly diminished TGFβ3 expression and GO-BP enrichment analysis showed a restraint of EMT. COL1A1, a member of the collagen family, was identified as a hub gene in the PPI network, whose dysregulation is thought to be associated with changes in the extracellular matrix and the subsequent metastasis of cancer cells(Theocharis et al., 2016). Studies also showed that the depression of COL1A1 could abrogate EMT and HCC stemness gene-signature(Ma et al., 2019). Besides mRNA-Seq analysis, qPCR and Western blot analysis also confirmed the down regulation of COL1A1 and N-Cadherin in AZ505-treated cells. Our findings suggest that SMYD2 inhibition accounted for TGFβ3 and COL1A1 downregulation and led to a restraint of EMT, which could partly explain the suppression of cell migration in AZ505-treated cells.

Accumulating evidence has indicated that SMYD2 is associated with the drug resistance in several cancers, including non-small cell lung cancer, renal cell carcinoma and colon cancer(Ren et al., 2019; Shang and Wei, 2019; Yan et al., 2019). Our results

showed that the inhibition of SMYD2 could significantly increase the sensitivity of chemo drugs in glioma cells. And the treatment of cisplatin could markedly reduce the expression SMYD2. The expression of proteins in cell is modulated by multiple regulatory mechanisms such as transcription, post-transcription, translation, and post-translational modification. Here, we found that the reduction of SMYD2 induced by cisplatin was modulated by STUB1. STUB1 was first discovered as a negative regulator of HSP70 and subsequent studies showed that STUB1 act as an E3 ubiquitin ligase participated the degradation of large number of proteins such as glucocorticoid receptor, polymerase β and DNA repair protein XRCC1(Connell et al., 2001; Parsons et al., 2008; Seo et al., 2019). STUB1 has been found to play inconsistent roles through different substrates. For example, STUB1 has been found to promote tumor via modulating the degradation of tumor suppressors including PTEN and MAPK(Ahmed et al., 2012; Kim et al., 2016), but attenuate malignancy of cancer through the degradation of oncogenes such as c-Myc, EGFR and ERBB2(Luan et al., 2018; Shi et al., 2020; Lin et al., 2021). Our results showed that higher STUB1 expression was associated with a better prognosis, and the knockdown of STUB1 could reverse the function of cisplatin. Thus, STUB1 may act as a tumor suppressor in glioma cells promoted drug sensitivity through the degradation of SMYD2.

In summary, our findings demonstrate that SMYD2 acted as a tumor promotor in gliomas and was a potential biomarker for the poor prognosis of glioma patients. Inhibition of SMYD2 suppressed the progression of glioma and improve drug sensitivity. Additionally, the treatment of cisplatin could significantly reduce the expression level of SMYD2 which was modulated by STUB1. On contrary to SMYD2, high expression of STUB1 was found to associated with a better prognosis in gliomas. And the suppression of STUB1 could reverse the function of cisplatin. Altogether, SMYD2 may serve as a new molecular diagnostic marker and therapeutic target for treating gliomas, and STUB1-SMYD2 pathway may be a putative target for reversing drug resistance in gliomas.

Ethics Statement

This study was carried out in accordance with the recommendations in the Guide for the

Care and Use of Laboratory Animals of the National Institutes of Health, and the corresponding protocol was approved by the Medical Ethics Committee of Jinhua Central Hospital (Jinhua, Zhejiang Province, China).

Author Contributions

KP: carried out the experiments and wrote the manuscript. BH: tissue microarray. LW: assisted with the experiments. JF: assisted with analyzed the experimental results. JY and WX: designed the experiments and modified the manuscript. All authors contributed to the article and approved the submitted version.

Funding

This work was supported by Key Research and Development Program of Zhejiang Province (2019C03044), Jinhua Science and Technology Research Program (2017-3-006, 2020-3-046, 2020-3-049), Natural Science Foundation of Zhejiang province (LY21H160014), Foundation of Jinhua hospital (JY2019-3-001, JY2020-6-04).

Conflict of Interest

The authors declare that the research was conducted in the absence of any commercial or financial relationships that could be construed as a potential conflict of interest.

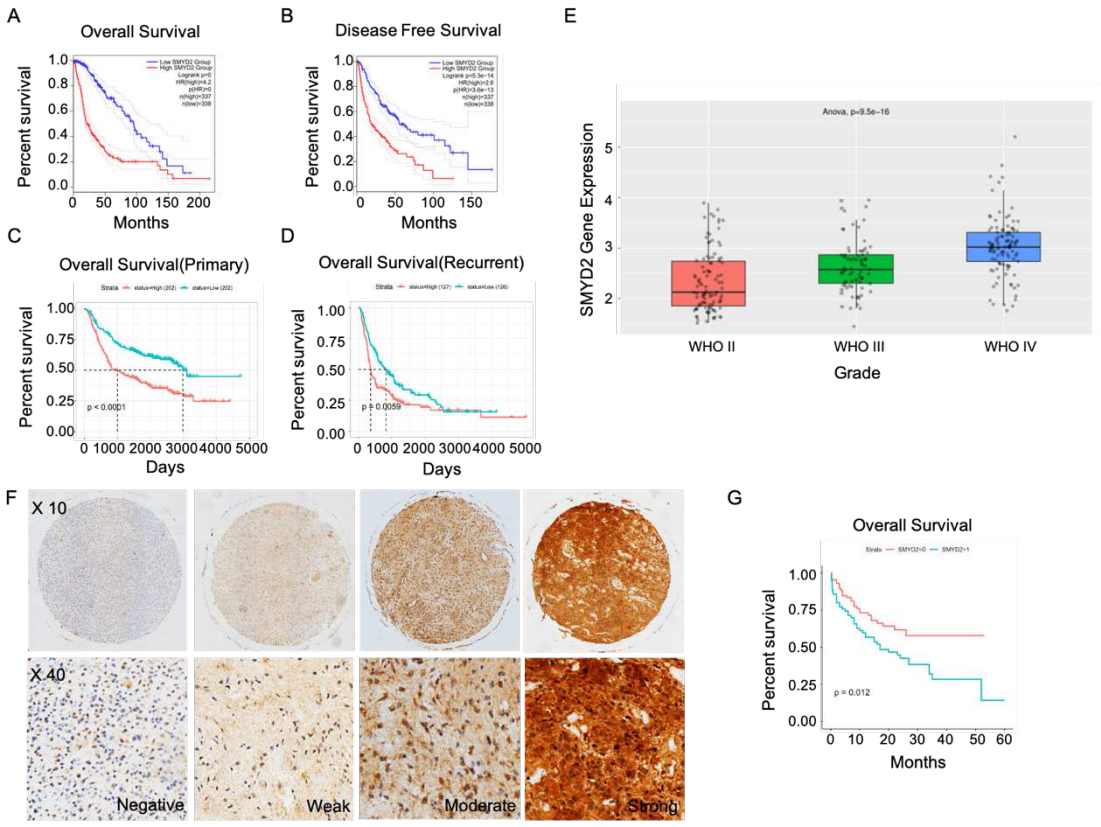

Fig1. SMYD2 expression was correlated with survival in glioma.

(A, B) Kaplan-Meier overall survival and disease-free survival curves based on the expression of SMYD2 from GEPIA database (P<0.0001 and P<0.0001, respectively). (C, D) Survival analysis in primary or recurrent glioma base on the mRNA level of SMYD2 from CGGA database (P<0.0001 and P=0.0059, respectively). (E) The expression of SMYD2 in different grade of glioma from CGGA database (P <0.0001). (F) Representative images SMYD2 immunohistochemical staining. From left to right they are: Negative, Weak, Moderate and Strong SMYD2 staining in glioma tissue. (G) Survival analysis of glioma patients according to the expression level of SMYD2 in 441 patients (P=0.012).

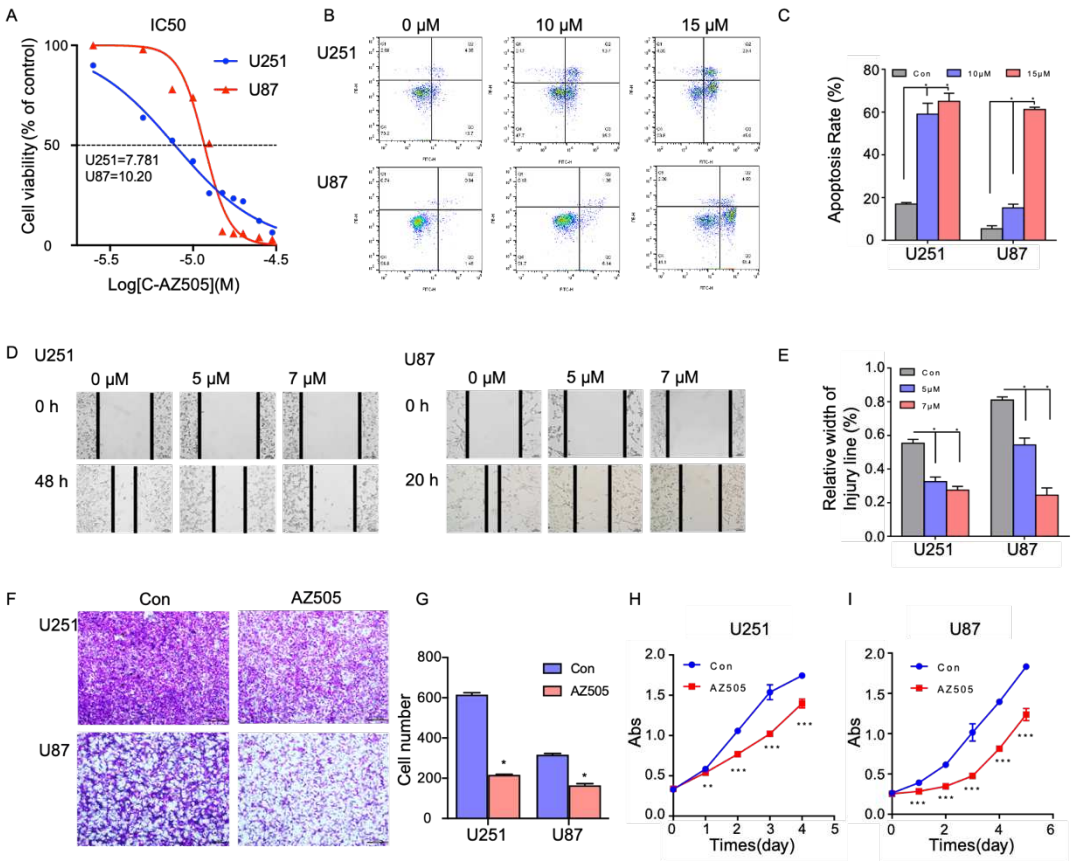

Fig2. SMYD2 inhibition suppressed cell proliferation and promoted cell apoptosis

(A) The IC50 of AZ505 in U251 and U87 cells. (B) Flow cytometric analysis following Annexin FITC and PI staining in AZ505-treated and control cells. (C) The apoptosis rate was quantified from three independent experiments. (D) Representative pictures of wound-healing assays in U251 and U87 cells with AZ505 treatment and controls. (E) Percentages of wound healing were calculated. (F) Representative pictures of migration in AZ505-treated and control cells. (G) Number of cell migration per field were counted in five random fields. (H-I) CCK-8 assays were performed to construct the growth curves of indicated cells. Data are shown as mean ± SD. *Compared to control group. $P < 0.05$.

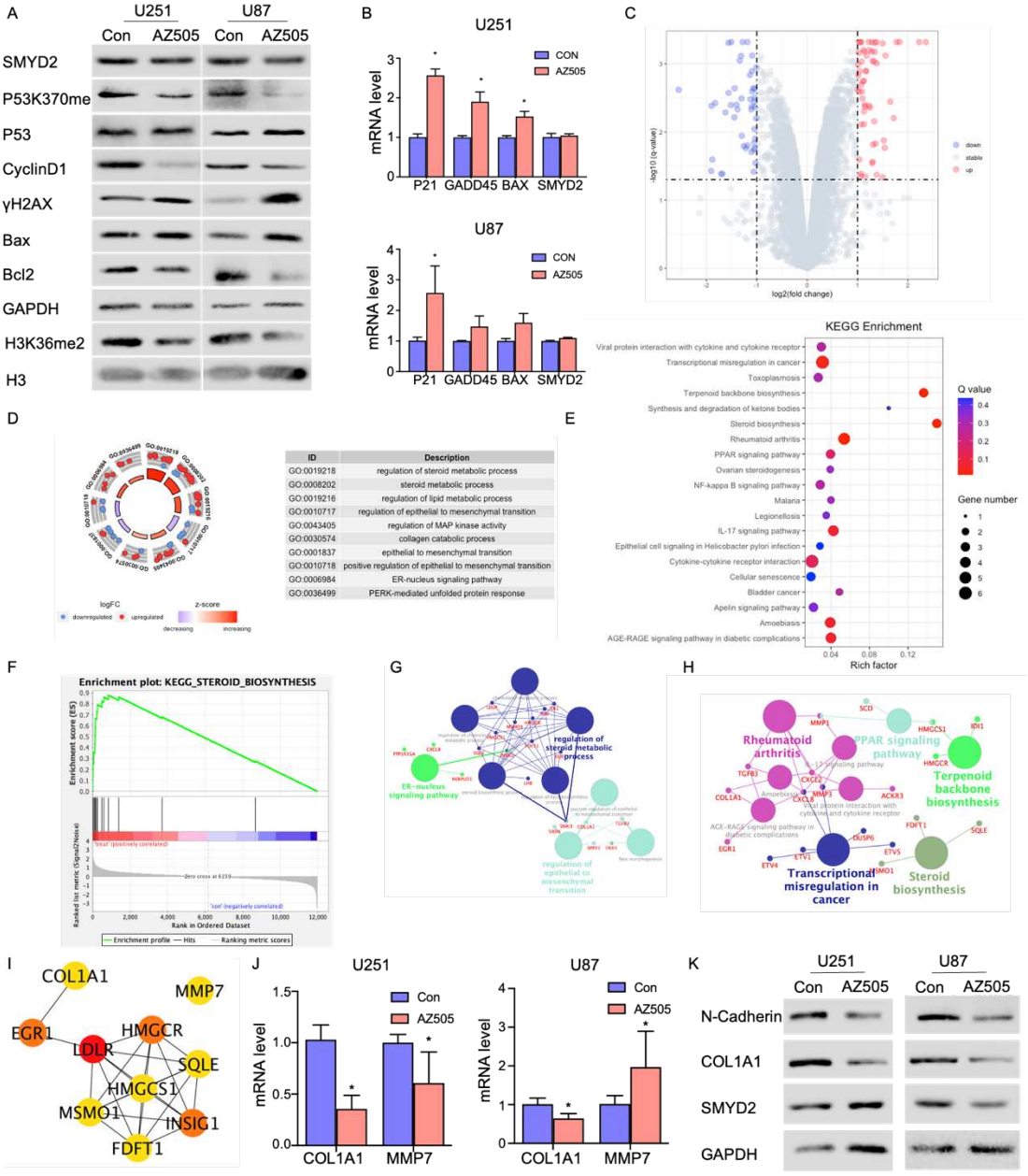

Fig. 3 The downstream mechanisms induced by SMYD2 inhibition.

(A) The expression levels of P53K370me, H3K36me2, CyclinD1, γH2AX, Bax and Bcl2 in AZ505-treated glioma cells. (B) The mRNA levels of P21, GADD45, Bax in AZ505-treated glioma cells. (C) Volcano plot of the differential expressed genes (DEGs) detected by mRNA sequencing. (D) GO annotations of DEGs with the top 10 enrichment scores of biological processes. Red dots represent upregulated genes; blue dots represent downregulated genes. The gradual size and color of rectangles in the middle represents the value of adjust P value and the regulation of genes in the enriched biological process, respectively. (E) KEGG enrichment analysis of DEGs. (F) GSEA analysis of detected

genes (FDR_qvalue<0.0001). (G-H) GO and KEGG enrichment analysis based on protein-protein interactions by ClueGo app of Cytoscape. (I)The top 10 hub genes of DEGs identified by degree algorithm of cytoHubba app. (J) Validation of the expression levels of COL1A1 and MMP7 using qPCR. (K) The expression levels of COL1A1 and N-Cadherin in AZ505-treated glioma cells. Data are shown as mean ± SD. * Compared to control group. P < 0.05.

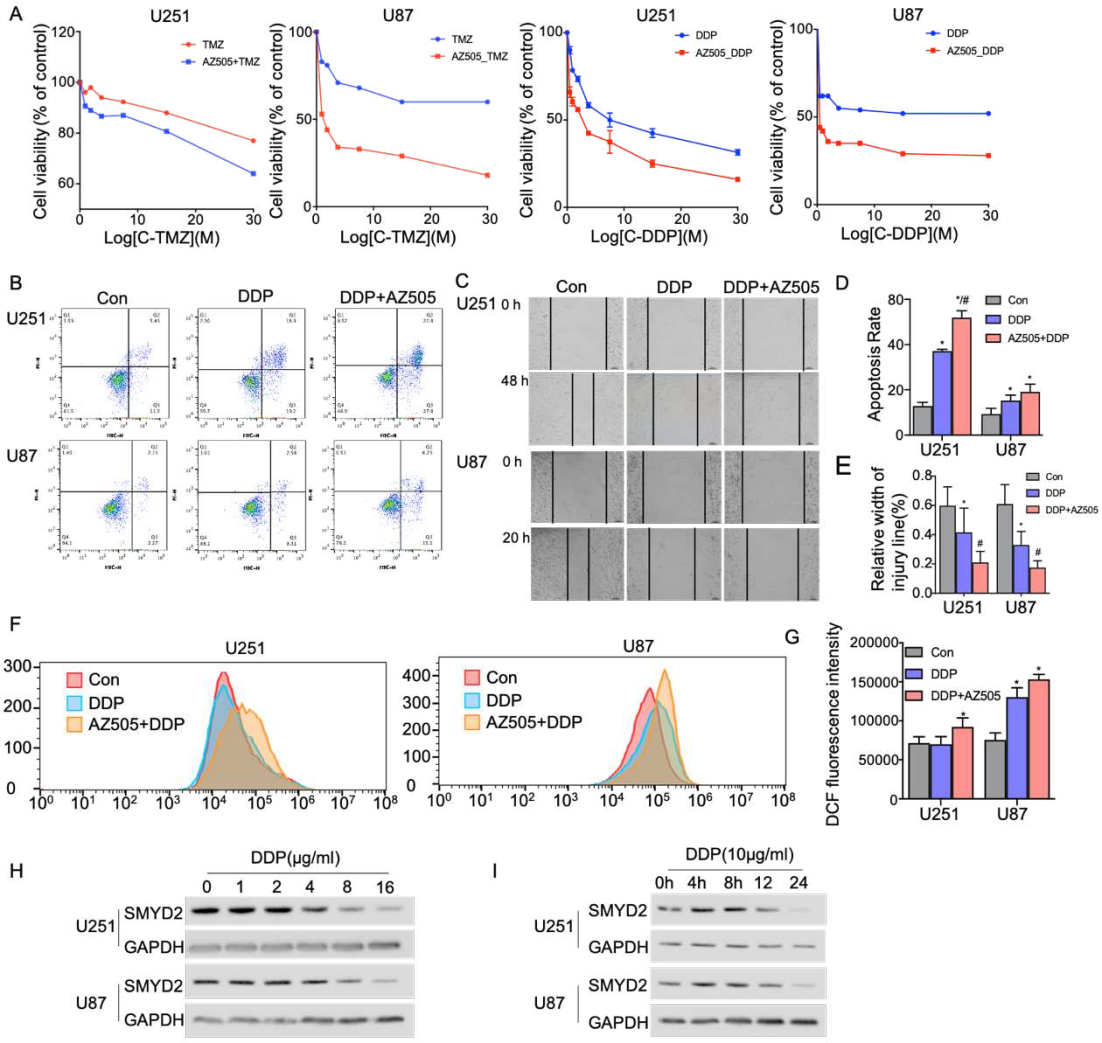

Fig. 4 Inhibition of SMYD2 enhanced drug sensitivity in glioma.

(A) The IC50 of TMZ and DDP in AZ505-treated and control cells. (B) Flow cytometric analysis in DDP, DDP combined AZ505 and control cells (C). Wound-healing assays in U251 and U87 cells with DDP, DDP combined AZ505 and control treatment. (D)The apoptosis rate was quantified. (E) Percentages of wound healing were calculated. (F) The reactive oxygen species assay in DDP, DDP combined AZ505-treated and control cells.

(G) The ROS rate was quantified. (H-I) The expression of SMYD2 in cells with different concentration and time of DDP treatment. Data are shown as mean ± SD. * Compared to control group. P < 0.05. # Compared to cisplatin-treated group. P<0.05.

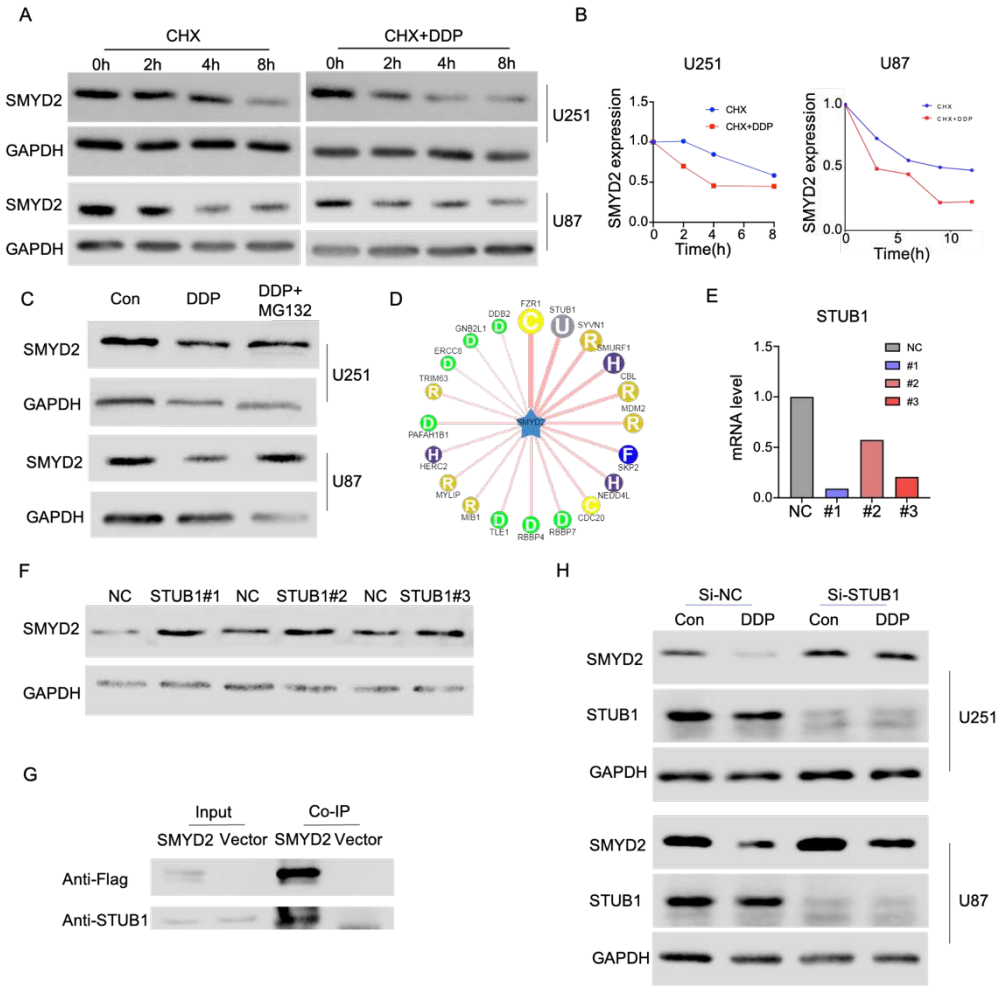

Fig. 5 STUB1 modulated SMYD2 degradation.

(A) SMYD2 protein levels at different time after DDP treatment in CHX-treated cells. (B) The degradation rate of SMYD2 was qualified. (C) SMYD2 protein levels in DDP, DDP combined MG132 and control cells. (D) The potential E3 ubiquitin ligases predicted in UbiBrowser. (E) STUB1 mRNA levels in si-RNA treated cells. (F) The expression of SMYD2 after the knockdown of STUB1. (G) Co-immunoprecipitation of SMYD2 and STUB1. (H)SMYD2 protein levels in DDP-treated and control cells after the knockdown of STUB1 or NC. Data are shown as mean ± SD. *P < 0.05.

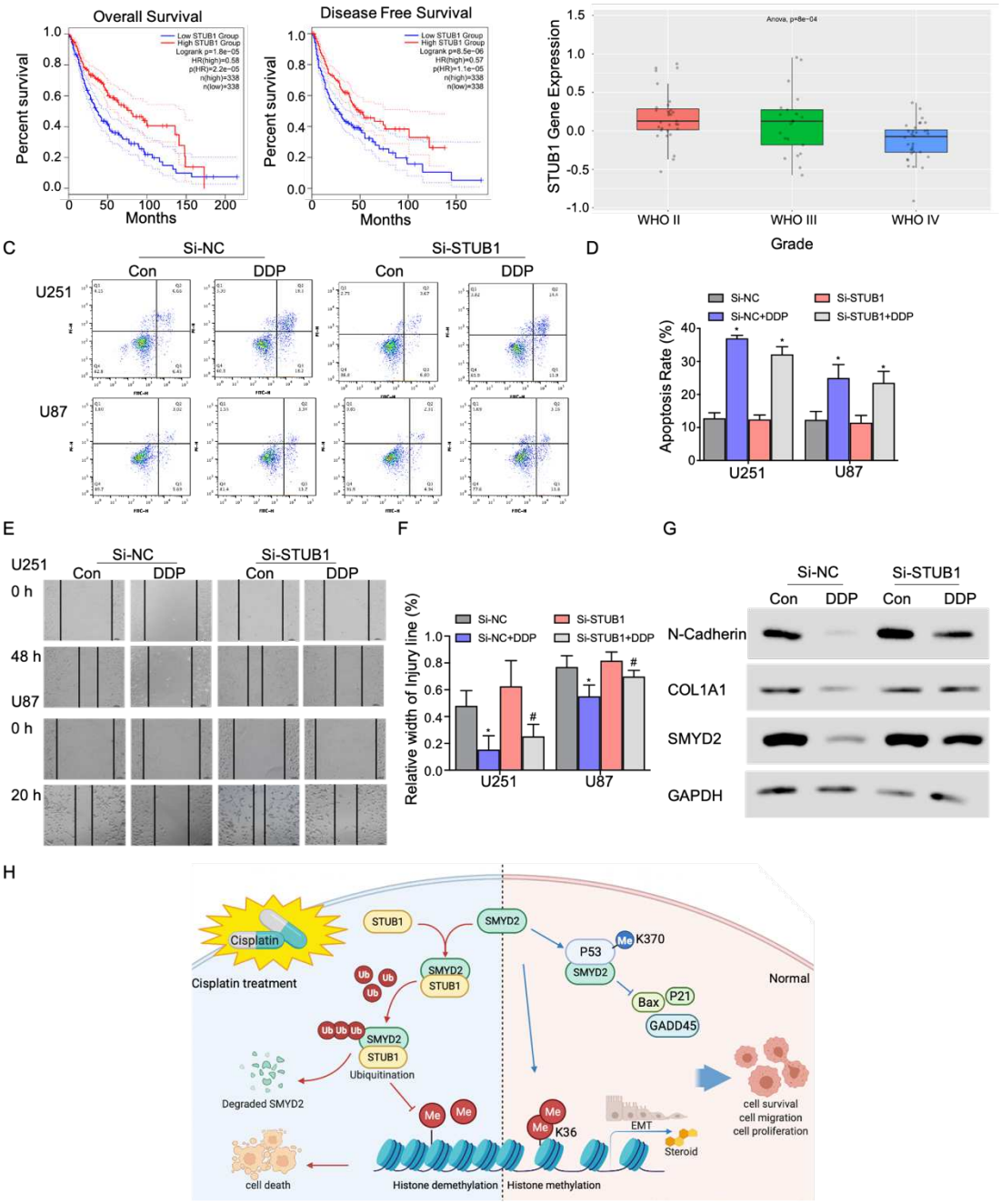

Fig. 6 STUB1 knockdown reverse the effect of cisplatin.

(A) Kaplan-Meier overall survival and disease-free survival curves based on the expression of STUB1 from GEPIA database (P<0.0001 and P<0.0001, respectively). (B) The expression of STUB1 in different grade of glioma from CGGA database (P <0.0001). (C) Flow cytometric analysis in DDP-treated and control cells after the knockdown of STUB1. (D) The apoptosis rate was quantified. (E) Would-healing assays in U251 and U87 cells with DDP-treated and control cells after STUB1 knockdown. (F) Percentages of wound healing were calculated. (G) The expression levels of COL1A1 and N-Cadherin in

different groups. (H) Hypothesis diagram. Data are shown as mean ± SD. * Compared to control group. P < 0.05. # Compared to cisplatin-treated group. P<0.05.

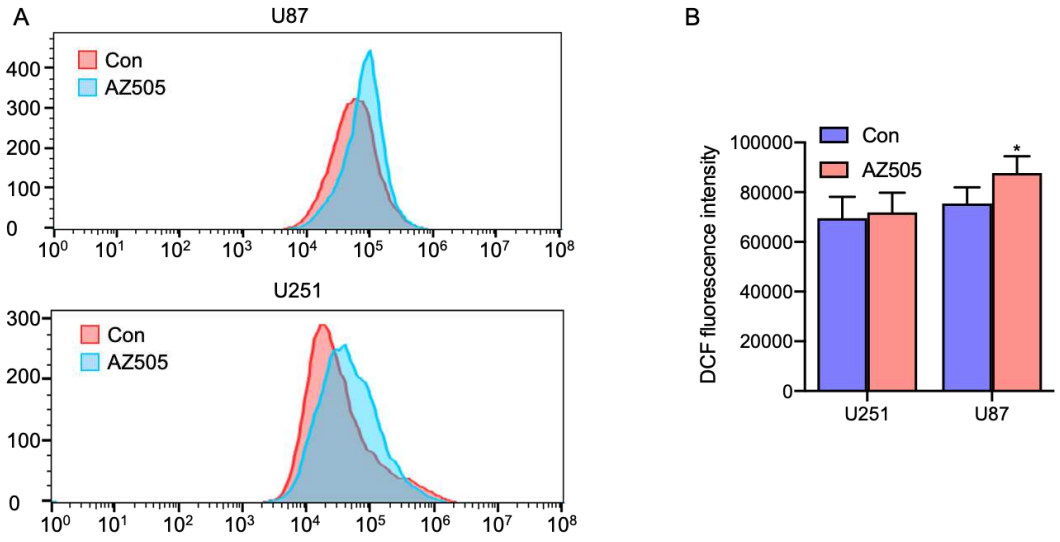

Fig. S1. The reactive oxygen species (ROS) assay in glioma cells.

(A) Flow cytometric analysis following DCFH-DA reaction in AZ505-treated U251 and U87 cells. (B)The ROS rate was qualified. Data are shown as mean ± SD. *P < 0.05.

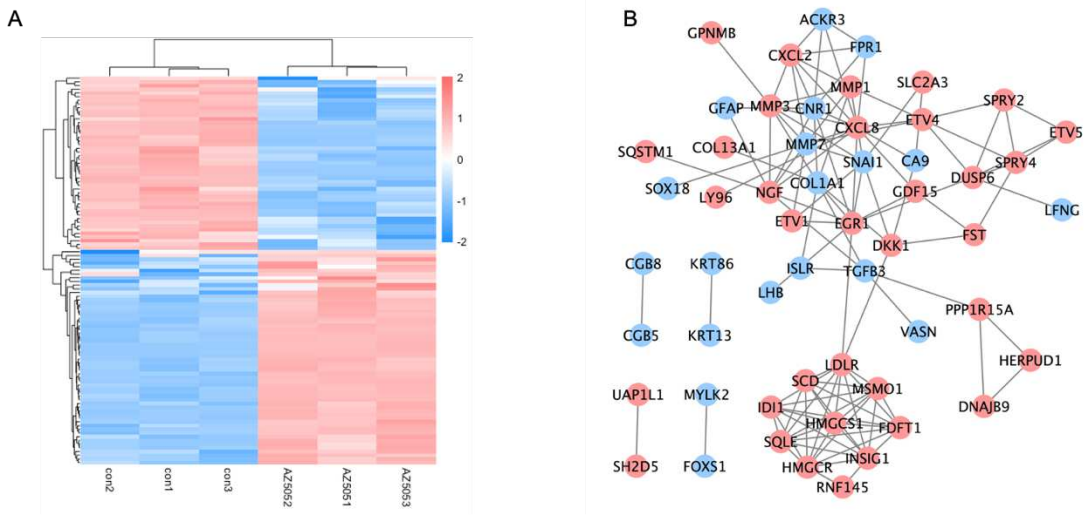

Fig. S2. The downstream mechanisms of SMYD2.

(A) Heat maps of significantly differentially expressed genes. (B) The PPI network of DEGs.

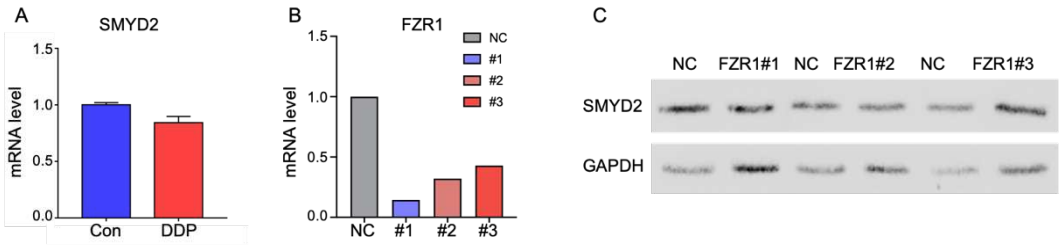

Fig. S3. The modulation of SMYD2 protein level.

(A) SMYD2 mRNA level in DDP-treated and control cells. (B) FZR1 mRNA levels in si-RNA treated cells. (C) The expression of SMYD2 after the knockdown of FZR1.

617

618 Table 1 SMYD2 staining and clinicopathological characteristics of 441 glioma patients.

variables	SMYD2 staining			
	Low (%)	High (%)	Total	P*
All cases	227(51.5)	214(48.5)	441	
Age				0.095
<=42 years	128(55.7)	102(44.3)	230	
>42 years	99(46.9)	112(53.1)	211	
Gender				0.66
Male	139(52.7)	125(47.3)	264	
Female	88(49.7)	89(50.3)	177	
WHO grade				0.004
I	25(67.6)	12(32.4)	37	
II	113(56.5)	87(43.5)	200	
III	57(47.1)	64(52.9)	121	
IV	27(36.5)	47(63.5)	74	
Histological type				0.168
Astrocytoma	178(55.5)	143(44.5)	321	
Glioblastoma	19(35.8)	34(64.2)	53	
Oligodendroglioma	13(44.8)	16(55.2)	29	
Ependymoma	2(40.0)	3(60.0)	5	
Medulloblastoma	5(31.3)	11(68.8)	16	

*Two-sided Fisher's exact tests

Some cases were not available for the information

619

620

621 Table 2 The Keplan-Meier survival analysis of hub genes in GEPIA2 database.

Top 10 ranked by Degree method

Rank	Name	Score	HR(OS)	P(OS)	HR(PFS)	P(PFS)	logFC	adj.P.Val	change
1	LDLR	10	0.91	0.46	0.85	0.18	1.377235879	0.00047918	up
2	HMGCR	9	0.48	3.40E-08	0.59	2.90E-05	1.118128314	0.000626303	up
2	INSIG1	9	0.53	2.10E-06	0.76	0.029	1.835558542	0.00047918	up
2	EGR1	9	2.2	3.30E-09	1.9	3.90E-07	1.079054844	0.002010849	up
5	FDFT1	8	0.46	3.10E-09	0.61	0.00011	1.028121871	0.00047918	up
5	MSMO1	8	0.57	2.20E-05	0.75	0.026	1.382276847	0.000981583	up
5	SQLE	8	0.77	0.044	0.81	0.089	1.18327639	0.000755102	up
5	HMGCS1	8	0.4	1.20E-11	0.48	1.20E-08	1.775466478	0.00047918	up
5	COL1A1	8	3.5	0	2.5	1.50E-12	-1.439526888	0.002285464	down
5	MMP7	8	3	1.10E-15	2.4	1.90E-11	-1.127173975	0.003321909	down

622

623

References

1. Ahmed, S.F., Deb, S., Paul, I., Chatterjee, A., Mandal, T., Chatterjee, U., et al. (2012). The chaperone-assisted E3 ligase C terminus of Hsc70-interacting protein (CHIP) targets PTEN for proteasomal degradation. *J Biol Chem* 287(19), 15996-16006. doi: 10.1074/jbc.M111.321083.

2. Brown, M.A., Sims, R.J., 3rd, Gottlieb, P.D., and Tucker, P.W. (2006). Identification and characterization of Smyd2: a split SET/MYND domain-containing histone H3 lysine 36-specific methyltransferase that interacts with the Sin3 histone deacetylase complex. *Mol Cancer* 5, 26. doi: 10.1186/1476-4598-5-26.

3. Chen, S., Kapilashrami, K., Senevirathne, C., Wang, Z., Wang, J., Linscott, J.A., et al. (2019). Substrate-Differentiated Transition States of SET7/9-Catalyzed Lysine Methylation. *J Am Chem Soc* 141(20), 8064-8067. doi: 10.1021/jacs.9b02553.

4. Cho, H.S., Hayami, S., Toyokawa, G., Maejima, K., Yamane, Y., Suzuki, T., et al. (2012). RB1 methylation by SMYD2 enhances cell cycle progression through an increase of RB1 phosphorylation. *Neoplasia* 14(6), 476-486. doi: 10.1593/neo.12656.

5. Connell, P., Ballinger, C.A., Jiang, J., Wu, Y., Thompson, L.J., Höhfeld, J., et al. (2001). The co-chaperone CHIP regulates protein triage decisions mediated by heat-shock proteins. *Nat Cell Biol* 3(1), 93-96. doi: 10.1038/35050618.

6. Du, B., and Shim, J.S. (2016). Targeting Epithelial-Mesenchymal Transition (EMT) to Overcome Drug Resistance in Cancer. *Molecules* 21(7). doi: 10.3390/molecules21070965.

7. Espinosa, G., López-Montero, I., Monroy, F., and Langevin, D. (2011). Shear rheology of lipid monolayers and insights on membrane fluidity. *Proc Natl Acad Sci U S A* 108(15), 6008-6013. doi: 10.1073/pnas.1018572108.

8. Ferguson, A.D., Larsen, N.A., Howard, T., Pollard, H., Green, I., Grande, C., et al. (2011). Structural basis of substrate methylation and inhibition of SMYD2. *Structure* 19(9), 1262-1273. doi: 10.1016/j.str.2011.06.011.

9. Göbel, A., Rauner, M., Hofbauer, L.C., and Rachner, T.D. (2020). Cholesterol and beyond - The role of the mevalonate pathway in cancer biology. *Biochim Biophys Acta Rev Cancer* 1873(2), 188351. doi: 10.1016/j.bbcan.2020.188351.

10. Gonzalez, D.M., and Medici, D. (2014). Signaling mechanisms of the

654 epithelial-mesenchymal transition. *Sci Signal* 7(344), re8. doi: 10.1126/scisignal.2005189.
655 11. Guo, D., Reinitz, F., Youssef, M., Hong, C., Nathanson, D., Akhavan, D., et al. (2011). An
656 LXR agonist promotes glioblastoma cell death through inhibition of an
657 EGFR/AKT/SREBP-1/LDLR-dependent pathway. *Cancer Discov* 1(5), 442-456. doi:
658 10.1158/2159-8290.Cd-11-0102.
659 12. Huang, J., Perez-Burgos, L., Placek, B.J., Sengupta, R., Richter, M., Dorsey, J.A., et al.
660 (2006). Repression of p53 activity by Smyd2-mediated methylation. *Nature* 444(7119),
661 629-632. doi: 10.1038/nature05287.
662 13. Ivanov, G.S., Ivanova, T., Kurash, J., Ivanov, A., Chuikov, S., Gizatullin, F., et al. (2007).
663 Methylation-acetylation interplay activates p53 in response to DNA damage. *Mol Cell Biol*
664 27(19), 6756-6769. doi: 10.1128/mcb.00460-07.
665 14. Kim, S.M., Grenert, J.P., Patterson, C., and Correia, M.A. (2016). CHIP(-/-)-Mouse Liver:
666 Adiponectin-AMPK-FOXO-Activation Overrides CYP2E1-Elicited JNK1-Activation, Delaying
667 Onset of NASH: Therapeutic Implications. *Sci Rep* 6, 29423. doi: 10.1038/srep29423.
668 15. Komatsu, S., Ichikawa, D., Hirajima, S., Nagata, H., Nishimura, Y., Kawaguchi, T., et al.
669 (2015). Overexpression of SMYD2 contributes to malignant outcome in gastric cancer. *Br J*
670 *Cancer* 112(2), 357-364. doi: 10.1038/bjc.2014.543.
671 16. Kukita, A., Sone, K., Oda, K., Hamamoto, R., Kaneko, S., Komatsu, M., et al. (2019).
672 Histone methyltransferase SMYD2 selective inhibitor LLY-507 in combination with poly ADP
673 ribose polymerase inhibitor has therapeutic potential against high-grade serous ovarian
674 carcinomas. *Biochem Biophys Res Commun* 513(2), 340-346. doi:
675 10.1016/j.bbrc.2019.03.155.
676 17. Lin, C.Y., Huang, K.Y., Lin, Y.C., Yang, S.C., Chung, W.C., Chang, Y.L., et al. (2021).
677 Vorinostat combined with brigatinib overcomes acquired resistance in EGFR-C797S-mutated
678 lung cancer. *Cancer Lett* 508, 76-91. doi: 10.1016/j.canlet.2021.03.022.
679 18. Luan, H., Mohapatra, B., Bielecki, T.A., Mushtaq, I., Mirza, S., Jennings, T.A., et al. (2018).
680 Loss of the Nuclear Pool of Ubiquitin Ligase CHIP/STUB1 in Breast Cancer Unleashes the
681 MZF1-Cathepsin Pro-oncogenic Program. *Cancer Res* 78(10), 2524-2535. doi:
682 10.1158/0008-5472.Can-16-2140.
683 19. Ma, H.P., Chang, H.L., Bamodu, O.A., Yadav, V.K., Huang, T.Y., Wu, A.T.H., et al. (2019).

684 Collagen 1A1 (COL1A1) Is a Reliable Biomarker and Putative Therapeutic Target for
685 Hepatocellular Carcinogenesis and Metastasis. *Cancers (Basel)* 11(6). doi:
686 10.3390/cancers11060786.
687 20. Nakakido, M., Deng, Z., Suzuki, T., Dohmae, N., Nakamura, Y., and Hamamoto, R. (2015).
688 Dysregulation of AKT Pathway by SMYD2-Mediated Lysine Methylation on PTEN. *Neoplasia*
689 17(4), 367-373. doi: 10.1016/j.neo.2015.03.002.
690 21. Ostrom, Q.T., Gittleman, H., Xu, J., Kromer, C., Wolinsky, Y., Kruchko, C., et al. (2016).
691 CBTRUS Statistical Report: Primary Brain and Other Central Nervous System Tumors
692 Diagnosed in the United States in 2009-2013. *Neuro Oncol* 18(suppl_5), v1-v75. doi:
693 10.1093/neuonc/now207.
694 22. Parsons, J.L., Tait, P.S., Finch, D., Dianova, II, Allinson, S.L., and Dianov, G.L. (2008).
695 CHIP-mediated degradation and DNA damage-dependent stabilization regulate base excision
696 repair proteins. *Mol Cell* 29(4), 477-487. doi: 10.1016/j.molcel.2007.12.027.
697 23. Qiu, Z., Yuan, W., Chen, T., Zhou, C., Liu, C., Huang, Y., et al. (2016). HMGCR positively
698 regulated the growth and migration of glioblastoma cells. *Gene* 576(1 Pt 1), 22-27. doi:
699 10.1016/j.gene.2015.09.067.
700 24. Ren, H., Wang, Z., Chen, Y., Liu, Y., Zhang, S., Zhang, T., et al. (2019). SMYD2-OE
701 promotes oxaliplatin resistance in colon cancer through MDR1/P-glycoprotein via
702 MEK/ERK/AP1 pathway. *Onco Targets Ther* 12, 2585-2594. doi: 10.2147/ott.S186806.
703 25. Saddic, L.A., West, L.E., Aslanian, A., Yates, J.R., 3rd, Rubin, S.M., Gozani, O., et al.
704 (2010). Methylation of the retinoblastoma tumor suppressor by SMYD2. *J Biol Chem* 285(48),
705 37733-37740. doi: 10.1074/jbc.M110.137612.
706 26. Seo, J., Han, S.Y., Seong, D., Han, H.J., and Song, J. (2019). Multifaceted C-terminus of
707 HSP70-interacting protein regulates tumorigenesis via protein quality control. *Arch Pharm Res*
708 42(1), 63-75. doi: 10.1007/s12272-018-1101-8.
709 27. Shang, L., and Wei, M. (2019). Inhibition of SMYD2 Sensitized Cisplatin to Resistant Cells
710 in NSCLC Through Activating p53 Pathway. *Front Oncol* 9, 306. doi:
711 10.3389/fonc.2019.00306.
712 28. Shi, W., Feng, L., Dong, S., Ning, Z., Hua, Y., Liu, L., et al. (2020). FBXL6 governs c-MYC
713 to promote hepatocellular carcinoma through ubiquitination and stabilization of HSP90AA1.

Cell Commun Signal 18(1), 100. doi: 10.1186/s12964-020-00604-y.

29. Song, J., Liu, Y., Chen, Q., Yang, J., Jiang, Z., Zhang, H., et al. (2019). Expression patterns and the prognostic value of the SMYD family members in human breast carcinoma using integrative bioinformatics analysis. *Oncol Lett* 17(4), 3851-3861. doi: 10.3892/ol.2019.10054.

30. Su, J., Morgani, S.M., David, C.J., Wang, Q., Er, E.E., Huang, Y.H., et al. (2020). TGF-β orchestrates fibrogenic and developmental EMTs via the RAS effector RREB1. *Nature* 577(7791), 566-571. doi: 10.1038/s41586-019-1897-5.

31. Sun, X.L., Lv, J.L., Dou, L., Chen, D., Zhu, Y.C., and Hu, X. (2020). LncRNA NEAT1 promotes cardiac hypertrophy through microRNA-19a-3p/SMYD2 axis. *Eur Rev Med Pharmacol Sci* 24(3), 1367-1377. doi: 10.26355/eurrev_202002_20194.

32. Tan, A.C., Ashley, D.M., López, G.Y., Malinzak, M., Friedman, H.S., and Khasraw, M. (2020). Management of glioblastoma: State of the art and future directions. *CA Cancer J Clin* 70(4), 299-312. doi: 10.3322/caac.21613.

33. Theocharis, A.D., Skandalis, S.S., Gialeli, C., and Karamanos, N.K. (2016). Extracellular matrix structure. *Adv Drug Deliv Rev* 97, 4-27. doi: 10.1016/j.addr.2015.11.001.

34. Tomiyama, A., and Ichimura, K. (2019). Signal transduction pathways and resistance to targeted therapies in glioma. *Semin Cancer Biol* 58, 118-129. doi: 10.1016/j.semcancer.2019.01.004.

35. Wang, D., Ma, L., Wang, B., Liu, J., and Wei, W. (2017). E3 ubiquitin ligases in cancer and implications for therapies. *Cancer Metastasis Rev* 36(4), 683-702. doi: 10.1007/s10555-017-9703-z.

36. Wang, H., Song, X., Liao, H., Wang, P., Zhang, Y., Che, L., et al. (2020a). Overexpression of SMAD7 activates the YAP/NOTCH cascade and promotes liver carcinogenesis in mice and humans. *Hepatology*. doi: 10.1002/hep.31692.

37. Wang, Q., Shi, L., Shi, K., Yuan, B., Cao, G., Kong, C., et al. (2020b). CircCSPP1 Functions as a ceRNA to Promote Colorectal Carcinoma Cell EMT and Liver Metastasis by Upregulating COL1A1. *Front Oncol* 10, 850. doi: 10.3389/fonc.2020.00850.

38. Wei, C.Y., Zhu, M.X., Yang, Y.W., Zhang, P.F., Yang, X., Peng, R., et al. (2019). Downregulation of RNF128 activates Wnt/β-catenin signaling to induce cellular EMT and

744 stemness via CD44 and CTTN ubiquitination in melanoma. *J Hematol Oncol* 12(1), 21. doi:
745 10.1186/s13045-019-0711-z.
746 39. Wijers, M., Kuivenhoven, J.A., and van de Sluis, B. (2015). The life cycle of the
747 low-density lipoprotein receptor: insights from cellular and in-vivo studies. *Curr Opin Lipidol*
748 26(2), 82-87. doi: 10.1097/mol.0000000000000157.
749 40. Xu, H., Zhou, S., Tang, Q., Xia, H., and Bi, F. (2020). Cholesterol metabolism: New
750 functions and therapeutic approaches in cancer. *Biochim Biophys Acta Rev Cancer* 1874(1),
751 188394. doi: 10.1016/j.bbcan.2020.188394.
752 41. Xu, W., Chen, F., Fei, X., Yang, X., and Lu, X. (2018). Overexpression of SET and MYND
753 Domain-Containing Protein 2 (SMYD2) Is Associated with Tumor Progression and Poor
754 Prognosis in Patients with Papillary Thyroid Carcinoma. *Med Sci Monit* 24, 7357-7365. doi:
755 10.12659/msm.910168.
756 42. Yan, L., Ding, B., Liu, H., Zhang, Y., Zeng, J., Hu, J., et al. (2019). Inhibition of SMYD2
757 suppresses tumor progression by down-regulating microRNA-125b and attenuates multi-drug
758 resistance in renal cell carcinoma. *Theranostics* 9(26), 8377-8391. doi: 10.7150/thno.37628.
759 43. Zhang, X., Tanaka, K., Yan, J., Li, J., Peng, D., Jiang, Y., et al. (2013). Regulation of
760 estrogen receptor α by histone methyltransferase SMYD2-mediated protein methylation. *Proc*
761 *Natl Acad Sci U S A* 110(43), 17284-17289. doi: 10.1073/pnas.1307959110.
762